Blocking FSH Induces Thermogenic Adipose Tissue and Reduces Body Fat

[1,2*]Yaoting Ji, [1*]Peng Liu, [1]Tony Yuen, [3]Elizabeth Rendina-Ruedy, [3]Victoria E. DeMambro, [1]Ping Lu, [1]Samarth Dhawan, [1]Wahid Abu-Amer, [1]Valeria Shnayder, [4]Bin Zhou, [1]Andrew Shin, [4]Samuel T. Robinson, [4]Yue Eric Yu, [1]Yu Zhou, [1]Ling-Ling Zhu, [3]Michaela R. Reagan, [1]Maria New, [5]Jay Cao, [4]Edward X. Guo, [6]Jameel Iqbal, [7]Henrik Molina, [8]Narayan G. Avadhani, [9]Shozeb Haider, [1,10]Marc Feldmann, [1]Christoph Buettner, [2]Bian Zhuan, [1#]Li Sun, [3#]Clifford J. Rosen, and [1#]Mone Zaidi ([*]joint first authors; [#]joint senior authors)

[1]Departments of Medicine, Pediatrics, and Structural and Chemical Biology, and The Mount Sinai Bone Program, Icahn School of Medicine at Mount Sinai, New York, NY 10029, USA

[2]School of Stomatology, Wuhan University, Wuhan, China

[3]Maine Medical Center Research Institute, Scarborough, Maine, ME 04074, USA

[4]Department of Biomechanical Engineering, Columbia University, New York, NY 10027, USA

[5]USDA Department of Agriculture, Human Nutrition Research Center, Fargo, North Dakota, ND 58203, USA

[6]Greater Los Angeles VA Medical Center, Los Angeles, CA 90073, USA

[7]Proteomics Resource Center, Rockefeller University, New York NY 10065, USA

[8]Department of Biomedical Sciences, University of Pennsylvania School of Veterinary Medicine, Philadelphia, PA 19104, USA

[9]Department of Computational Chemistry, University College London School of Pharmacy, London WC1N 1AX, UK

[10]Kennedy Institute of Rheumatology, Oxford University, Oxford OX1 2JD, UK

Correspondence and request for materials should be addressed to:

mone.zaidi@mssm.edu

ABSTRACT

Menopause is associated with bone loss and visceral adiposity. Although estrogen prevents bone loss, its inhibitory effect on body fat is less consistent. We questioned instead whether we could target a rising Fsh level during the perimenopausal transition with a single agent to increase bone mass and reduce body fat. We previously showed that a polyclonal antibody (Ab) that binds to the β-subunit of Fsh and blocks its interaction with the Fsh receptor (Fshr) increases bone mass. Here, we report that the Fsh Ab causes a marked reduction in visceral white adipose tissue (WAT) in mice fed a high fat diet, in ovariectomized mice, and interestingly, in mice on normal chow. The global reduction in body fat, not seen in *Fshr*$^{-/-}$ mice that were similarly treated with Ab, was associated with profound beiging and brown adipose tissue (BAT) activation, noted most impressively in the ThermoMouse, in which *Luc2* is driven by an *Ucp1* promoter. These changes were accompanied by increased indices of thermogenesis, namely energy expenditure, oxygen utilization and physical activity, as well as increased mitochondrial density noted in the PhAM^{excised} mouse. We show that these actions result from the specific binding of Ab to Fshβ to block its action on full-length, signaling-efficient Fshrs abundantly expressed in adipocytes. Our studies expose novel opportunities for treating both obesity and osteoporosis.

Fsh favors mammalian procreation by synthesizing and releasing estrogen from ovarian follicles, where Fsh receptors (Fshrs) are highly expressed. However, it is not inconceivable that Fsh, through its action on the skeleton[1], may also regulate intergenerational calcium transfer from the mother to mineralize the offspring's skeleton. Whereas there is no evidence yet for this action, what is clear is that FSH levels become elevated as the ability to procreate ceases at menopause. It is during the late perimenopause, a period characterized by relatively stable estrogen and rising FSH levels, that bone loss occurs at its most rapid rate[2,3]. There is also a sharp increase in visceral adiposity during this life stage, which coincides with the emergence of disrupted energy balance and reduced physical activity[4]. While the subsequent decline in estrogen explains menopausal bone loss in large part[5], effects of estrogen deprivation on whole body metabolism remain unclear[6]. We therefore questioned whether, by targeting FSH, we could not only prevent bone loss, but also reduce visceral adiposity and improve energy homeostasis.

Fsh Ab Binds and Blocks Fsh Action in the Circulation

Considering that Fshr activation on osteoclasts enhanced bone resorption and that Fsh haploinsufficiency in the *Fshβ*$^{+/-}$ mouse was associated with low resorption rates and high bone mass[1], we raised a polyclonal antibody (Ab) to a 13-amino acid sequence of Fshβ (LVYKDPARPKIQK) that would, based on computational modeling, block Fsh binding to the Fshr[1,7,8]. As predicted, we found that the Ab inhibited bone resorption, stimulated new bone synthesis and increased bone mass in ovariectomized mice[7]. Here, we establish definitively that the Fsh Ab binds to and interrupts the

interaction of Fshβ with its receptor at concentrations well within the relevant circulating range.

Recombinant mouse Fsh (Fshα-Fshβ chimera, 2 µg) was passed through resin (Pierce Co-Immunoprecipitation Kit) with immobilized Fsh Ab or goat IgG. The elution, flow-through and wash fractions were then immunoblotted with a different Fsh Ab (Hf2). Figure 1A shows a band at the expected size, ~50 kD, in both elution and flow through fractions. In contrast, the eluted fraction from immobilized IgG did not display a band; instead, all protein appeared in the flow through fraction (Figure 1A). The Ab-immunoprecipitated eluate was trypsinized and analyzed by liquid chromatography tandem mass spectrometry (LC MS/MS), which matched ten peptides corresponding to the Fshα-Fshβ chimera (Figure 1B, Extended Data Table 1). This definitively established Fsh as the binding partner of the Ab.

We questioned whether the binding of the Ab to the LVYKDPARPKIQK sequence of human Fshβ, against which it was raised[7], could block the interaction of Fsh with the Fshr in mice. For this, we used the crystal structure of the human FSH-FSHR complex containing the LVYKDPARPKIQK sequence (PDB ID 4AY9) (Figure 1Ci) to model mouse Fsh(LVYKDPARPNTQK)-Fshr interactions *in silico* (Figure 1Cii). Binding modes of the respective complexes were found to be identical (*c.f.* Figures 1Ci and 1Cii). We further noted that the net positive charge of the peptide surface (blue residues) complements the overall negative charge of Fshr-binding surface (red residues), thus generating strong electrostatic interactions (Figure 1Ciii). Furthermore, and importantly, the loop from Fshβ (yellow) containing the peptide sequence tucked into a small groove generated by the Fshr (Figure 1Civ). We therefore predicted that

binding of an Ab to this sequence will inevitably block access of Fshβ to the small Fshr-binding groove, thus preventing ligand-receptor interaction.

Blockade of Fsh action by Ab was proven experimentally – the Ab reversed the Fsh-induced inhibition of *Ucp1*, a master regulator of adipocyte beiging[9,10]. For this, we used immortalized dedifferentiated brown adipocytes from the ThermoMouse (hereafter termed Thermo cells), in which the *Ucp1* promoter drives a *Luc2-T2A-tdTomato* reporter (Figure 1D)[11]. Exogenous Fsh (30 ng/mL) inhibited Luc2 activity in serum-free medium (devoid of Fsh) irrespective of the Arb3 agonist CL316243 (10^{-7} M) (Figure 1D). The Ab reversed this inhibition in a concentration-dependent manner, with complete reversal of the inhibition at 1 μg/mL Ab (Figure 1D).

We explored whether concentrations of Ab achieved in plasma following injection were sufficient to block the inhibition of *Ucp1* expression by Fsh. Specifically, we asked whether a serum concentration of at least 1 μg/mL resulted from a single i.p. injection of 100 μg Ab. ELISA-based measurements in mice injected with Ab revealed a sharp increase in plasma Fsh Ab, measured as goat IgG, at 2 hours and levels remained at $\geq$10 μg/mL up to at least 24 hours ($t_{1/2}$ = 25.6 hours) (Figure 1E). Thus, circulating Ab concentrations post-injection were at least 10-fold higher than those required for the inhibition of *Ucp1* by circulating Fsh.

Fsh Ab Reduces Adiposity and Induces Thermogenesis in Mice on High Fat Diet

Experiments using the Fsh Ab were carried out independently at the laboratories of M.Z. and C.J.R. (details in Extended Data Table 2). Both labs concurrently examined

the effect of Fsh Ab or goat IgG, injected at 200 μg/day, i.p., on white adipose tissue (WAT) accumulation in wild type C56BL/6 mice that were pair-fed or allowed *ad libitum* access to a high fat diet. Figure 2A shows equal food intake and no significant change in body weight with Ab treatment compared with goat IgG. Quantitative NMR (qNMR) showed a reduction in total body fat and fat mass/total mass (FM/TM), and an increase in lean mass/total mass (LM/TM) in mice treated with Ab for ~8 weeks compared with IgG (Figure 2B). Data were reproduced using both qNMR and dual energy X-ray absorptiometry (DXA) at 7 weeks, with no difference at 4 weeks (Figures 2B and 2C). DXA also showed a significant increase in bone mineral density at both 4 and 7 weeks (Figure 2D), in part explaining the increased lean mass in Ab-treated mice (*c.f.* Figure 2B).

Examination of the effect of Ab on distinct WAT compartments revealed highly significant decreases in adiposity, observed visually in coronal and transverse sections, on micro-computed tomography (μCT) of the entire thoracoabdominal cavity. Total fat volume (TFV), subcutaneous fat volume (SFV) and visceral fat volume (VFV) were all significantly lower in Ab- *versus* IgG-treated group (Figure 2E). Tissue weights, measured independently, showed decrements in inguinal (iWAT) and gonadal adipose tissue (gWAT) in Ab- compared with IgG-treated mice; no difference was observed in interscapular brown adipose tissue (BAT) (Figure 2F). Liver and skeletal muscle sections likewise showed decreased Oil Red-O staining, indicative of reduced fat accumulation with Ab (Figure 2G). Overall, despite equal food intake, the data show that Fsh inhibition with an Ab markedly reduces adiposity in all WAT compartments.

We performed indirect calorimetry using metabolic cages to determine the effects of Ab or IgG on whole body energy parameters, including O_2 consumption (VO_2), energy expenditure (EE), respiratory quotient (RQ), beam breaks (Xbreaks), walking distance and walking speed (Figure 2H). Indicative of a potent thermogenic response, Ab-treated mice showed increases in VO_2, EE, Xbreaks, and walking distance and speed at near-equal food intakes (Figure 2H). These findings, together with the sharply reduced WAT, appear consistent with the induction of thermogenic beige adipose tissue.

Glucose tolerance testing revealed no significant difference with Ab (Figure 2I). Consistent with this, plasma C-peptide levels were unchanged, as were plasma adiponectin and leptin levels (Figure 2J). Circulating total cholesterol and free fatty acids were also not significantly different, but there was an increase in plasma triglycerides in Ab-treated mice (Figure 2K).

Importantly, to probe whether the aforementioned anti-adiposity actions of the Ab were mediated solely through the Fsh axis *in vivo*, *Fshr*-deficient male mice were pair-fed on high fat diet and treated similarly with Ab (Figure 2L). Injection of wild type ($Fshr^{+/+}$) mice with Ab evoked an expected reduction in fat mass and an increase in lean mass (qNMR) (Figure 2M, *c.f.* Figure 2B). However, there was a graded reduction of this response with decreasing *Fshr* gene dosage, with no significant change in either parameter in $Fshr^{-/-}$ mice (Figure 2M). The observation that the Fsh Ab failed to reduce body fat in *Fshr*–deficient mice provides proof of Ab specificity *in vivo*.

Fsh Ab Reduces Adiposity and Induces Thermogenesis in Ovariectomized Mice Fed a Normal Diet

The perimenopausal transition is associated with increases in total body fat and decrements in energy expenditure and physical activity, all of which impact quality of life[4]. This clinical phenotype is recapitulated in rodents post-ovariectomy, as well as in chronic hypoestrogenemic models, such as in *Erα*$^{-/-}$, *aromatase*$^{-/-}$ and *Fshr*$^{-/-}$ mice[6,12-14]. While genetic Fshr deficiency does not seem to protect against the pro-adiposity effects of severe chronic hypoestrogenemia, we questioned whether acute suppression of Fsh action by an Fsh Ab can, through parallel mechanisms, not only attenuate bone loss[7], but also reduce body fat and improve energy homeostasis. Clinically, this is important during the late perimenopause, when the onset of central adiposity is accompanied by no change in estrogen and increases in Fsh levels[2].

We pair-fed mice with normal chow, so that their food intake was identical over 8 weeks of treatment with Fsh Ab or IgG given i.p. post-ovariectomy or sham-operation (Figure 3A). As with mice fed on a high fat diet (Figure 2A), total body weight remained unchanged (Figure 3A). Ovariectomy expectedly resulted in a significant increase in plasma Fsh levels (Figure 3B). To ensure that a higher circulating Fsh is blocked effectively, we used 200 or 400 μg/mouse of Ab in the ovariectomy group, as opposed to a 100 μg/mouse dose in sham-operated group. Of note, despite Fsh being bound to our Ab, which detects a small Fshr-binding sequence (Figure 1B) and blocks Fsh action on the Fshr (Figures 1C and 1D), total plasma Fsh levels measured by ELISA were not significantly different between Ab- and IgG-treated groups (Figure 3B). This confirms our previous data that the Fsh Ab does not in any significant way interfere with the

190 detection of Fsh by the ELISA kit[7]. Also, as noted previously[7], serum estrogen levels
191 remained unchanged with Ab treatment (Figure 3B).

192 Quantitative NMR showed a highly significant reduction in fat mass and FM/TM,
193 with an increase in LM/TM with Fsh Ab in both the sham-operated and ovariectomized
194 groups (Figure 3C, *c.f.* Figure 2B). In separate experiments, ovariectomized and sham-
195 operated mice on normal chow *ad libitum* were subject to abdominal μCT. Ab reduced
196 TFV, VFV and SFV significantly, not only in the ovariectomized group, but also in sham-
197 operated mice (Figure 3D). We also studied Ab effects on bone marrow adiposity using
198 osmium μCT. There was a clear decrease in marrow fat content (white) on visual
199 inspection in Ab-treated groups compared with IgG controls (Figure 3E). Quantitation
200 revealed that, in mainly diaphyseal voxels of interest (VOI), ovariectomy predictably
201 enhanced bone marrow adiposity (Figure 3E), and Ab decreased adiposity in all VOIs,
202 both in sham-operated and ovariectomized mice compared with their respective IgG
203 controls (Figure 3E). Indirect calorimetry showed that the Fsh Ab not only enhanced
204 resting and active EE, but also reduced RQ in both sham-operated and ovariectomized
205 mice (Figure 3F). There were no differences in plasma levels of glucose, cholesterol,
206 triglyceride or free fatty acids between any of the groups (Figure 3G).

207 It was most interesting, however, that sham-operated mice were equally
208 responsive to Ab. We thus repeated the study using 3 month-old C57BL/6 mice that
209 were either pair-fed or reverse pair-fed with normal chow (see Methods for details). Ab
210 reduced fat mass and FM/TM (qNMR), as well as abdominal TFV, SFV and VFV (μCT)
211 in both pair-fed and reverse pair-fed groups (Figure 4). Importantly, despite their
212 increase in caloric intake evident on reverse pair-feeding (Figure 4D), Ab-treated mice

showed a reduction in whole body and abdominal adiposity (Figures 4E, F). No changes in total body weight were noted in any of the four groups (Figure 4A, D). That Fsh inhibition by Ab in otherwise unperturbed mice resulted in reduced adiposity suggests that Fsh exerts a physiologic role in regulating body composition.

Blocking Fsh Action on Adipocyte Fshrs Induces *Ucp1* Expression

Fshr cDNA and protein has been identified on fat tissue and adipocytes[15,16], as well as by us, on osteoclasts and mesenchymal stem cells[1,7]. The receptors have been shown to couple with a G_i protein, the activation of which was found to reduce cAMP levels[1,15] and stimulate lipogenesis in 3T3.L1 cells[15,16]. Here, we document Fshr protein expression not only on 3T3.L1 cells, but also on Thermo cells and adipocytes derived from murine mesenchymal stem cells (MSC-ad), as well as, importantly, on murine BAT and inguinal and visceral WAT (Figures 5A, B). We have further Sanger sequenced full-length Fshr cDNA from MSC-ad and 3T3.L1 cells (Extended Data Figures 1, 2). Of note, despite the absence of exon 2 in adipocytes derived from 3T3.L1 cells, the Fshr remains signaling-efficient and is fully functional, particularly in its ability to stimulate the core lipogenic gene program (*Pparγ*, *Fas*, *Glut4*, *Lpl*, *Pref1*, and *Cebpd*) (Figure 5C). As further genetic evidence for Fsh effects on lipogenesis[15], we show that mesenchymal stem cells from *Fshr*$^{-/-}$ mice display reduced Oil Red-O staining (Figure 5D).

The mitochondrial protein Ucp1 has been widely recognized as a master regulator of white-to-beige transition of adipocytes[17]. We explored whether Fsh inhibited induction of Ucp1 using Thermo cells, wherein Luc2 radiance is measured as a Ucp1 surrogate (ref. Figure 1D). Experiments in the presence of serum, which contains

Fsh at 15-40 ng/mL (Figure 3B)[18], showed that the Ab (100 ng/mL) induced Ucp1 (Luc2) expression, irrespective of the addition of a known Ucp1 inducer, the Arb3 agonist CL316243 (Figure 5E). This stimulation was reversed by the further addition of Fsh (30 ng/mL), establishing Fsh specificity (Figure 5E, *c.f.* Figure 1D).

To examine the *in vivo* relevance of Ab effects on *Ucp1* activation, we implanted Thermo cells into both flanks of 3 month-old *nu/nu* mice and injected IgG or Ab (100 µg/mouse/day) for 2 months. A dramatic increase in total (from both flanks) and average Luc2 radiance was noted upon injection of D-Luciferin (Figure 5F). For confirmation, we examined tdTomato fluorescence (red) in iWAT sections. Consistent with enhanced Luc2 radiance, Ab-treated mice showed a marked increase in tdTomato expression (Figure 5G). Together, the data suggest that the Ab, by blocking Fsh action on the Fshr, activates *Ucp1*.

Fsh Ab Induces Thermogenic Adipose Tissue and Triggers BAT Activation

The induction of thermogenic adipose tissue, *a.k.a.* beiging, is typically characterized by the conversion of large lipid-rich adipocytes to significantly smaller, mitochondria-rich, energy-dissipating beige adipocytes that express *Ucp1* and other mitochondrial genes[17,19,20]. To determine whether the Fsh Ab induces thermogenic adipose tissue *in vivo*, wild type mice pair-fed on high fat diet or normal chow were injected with Ab or IgG in separate experiments.

Consistent with the induction of adipocyte beiging, there was a significant decrease in adipocyte area and perimeter in hematoxylin-stained sections of inguinal fat

pads from Ab-treated mice (Figure 6A). This was accompanied by a marked increase in Ucp1 immunostaining both in iWAT and BAT compartments (Figure 6B), as well as significant increases in the expression in iWAT of most brown fat genes, including *Ucp1*, *Cox7*, *Cidea*, *Cox8a*, *Lhx8*, *Lep*, *Irs1*, *Cebpb*, *Fabp4*, *Vegfa*, *Cebpa*, *Retn,* and *Retnla* (Figure 6C). Increases were also noted in *Ucp1*, *Cidea*, *Cebpa*, and *Vegfa* expression in BAT at 1 month, commensurate with the early activation of the BAT gene program (Figure 6C).

As a complementary *in vivo* test for early BAT activation and white-to-beige transition, and to examine the time courses of the respective effects, we imaged live ThermoMice (Figure 7), in which, as noted above (Figure 1D), a transgenic *Ucp1* promoter drives the *Luc2-T2A-tdTomato* reporter construct. This allows Luc2 radiance monitored *in vivo* to serve as a surrogate for *Ucp1* expression[11]. ThermoMice were pair-fed on a high fat diet and injected with Ab or IgG (100 µg/mouse/day). At 2 and 8 weeks, we measured Luc2 radiance emitted from both dorsal and ventral surfaces for optimal visualization of interscapular BAT and inguinal WAT, respectively.

Uninjected control mice showed no emitted radiance at either time point. At 2 weeks, there was a significant enhancement of Luc2 radiance emitted from interscapular BAT-rich region, and very little, if any, radiance from the iWAT-rich region (Figure 7A). The BAT signal intensity was significantly enhanced at 8 weeks. Furthermore, there was a marked ~3-fold difference in BAT radiance in Ab- *versus* IgG-treated mice (Figure 7B). A similarly dramatic difference in iWAT radiance was noted between Ab- and IgG-treated groups, particularly noted on ventral sampling (Figure 7B).

The data together confirm that the Ab triggers early BAT activation, which is followed by a slower induction of beiging in the WAT compartment.

Beiging is also associated with an increase in the density of functionally thermogenic mitochondria[21,22]. To assess for increased mitochondrial density, we used the PhAM^{excised} mouse, in which a fluorescent protein from the octocoral *Dendronephthya,* Dendra2, is fused to a Cox8 mitochondrial targeting signal, yielding mito-Dendra2 (Figure 7C)[23]. The expression of mito-Dendra2 thus reflects mitochondrial density. We analyzed frozen sections of sWAT, vWAT and BAT from PhAM^{excised} mice treated with Ab or IgG (200 µg/mouse/day) for 4 weeks. Compared with the IgG group, Ab-treated mice displayed a dramatic increase in mito-Dendra2 fluorescence in all compartments, and smaller, more condensed, adipocytes in WAT compartments (Figure 7C). This provided independent confirmation that Fsh inhibition induced mitochondria-rich, thermogenic adipose tissue.

DISCUSSION

The long-held belief that pituitary hormones act solely on master targets was first questioned when we documented G protein-coupled receptors for thyroid stimulating hormone (Tsh), Fsh, adrenocorticotrophic hormone (Acth), oxytocin and vasopressin on bone cells[1,24-29]. These evolutionarily conserved hormones and their receptors are known to have primitive roles, and exist in invertebrate species as far down as coelenterates[30]. It is not surprising therefore that each such hormone has multiple *hitherto* unrecognized functions in mammalian integrative physiology, and hence, becomes a potential target for therapeutic intervention.

Here, we show that blocking the access of Fsh to its receptor using an Ab results not only in increased bone mass, documented earlier[7], but also in a remarkable reduction in adiposity in mice on a high fat diet or following ovariectomy. This is coupled with the production of mitochondria-rich, thermogenic adipose tissue. Notably, the anti-adiposity effects of Ab *in vivo* are abrogated in *Fshr*$^{-/-}$ mice, proving that the Ab acts by inhibiting Fsh action. Furthermore, and importantly, that the Ab reduces adiposity in unperturbed mice on normal chow, suggests a physiologic role for Fsh in regulating body composition. Underscoring Fsh action, and confirming prior data[11,17], is the abundance of signaling-efficient Fshrs on adipocytes at all stages of differentiation. Fsh acts on these receptors to inhibit *Ucp1* activation, and our Ab causes a dramatic, time-dependent increase in *Ucp1* in both BAT and WAT compartments *in vivo.* The latter action, best observed in the ThermoMouse, is associated with effects characteristic of thermogenic adipose tissue induction, namely alterations in cell morphology, gene expression, and mitochondrial density.

Previous human studies and particularly the Study of Women's Health Across the Nations (SWAN), an observational cohort of pre-, peri, and postmenopausal women followed over several years, showed that a phase of rapid bone loss ensues two to three years prior to the onset of menopause when FSH levels are rising and estrogen is relatively stable[2,3]. SWAN also documented a better correlation of serum FSH with bone loss than declining estrogen levels[3]. Furthermore, even after the onset of menopause, estrogen replacement therapy does not suppress serum FSH levels into the premenopausal range[31], and women often continue to lose bone and further accrue visceral fat. Our study supports these tenets, but more importantly provides

mechanistic insights into the clinical problem of peri- and postmenopausal weight gain and disrupted energy balance[4,6].

The use of agents to prevent weight gain or treat obesity, consisting mainly of those that reduce appetite or inhibit nutrient absorption, is compromised by issues of poor efficacy and unacceptable side effects[19]. Thus, the therapeutic armamentarium for obesity pales in comparison with that of other public health hazards of similar or even lesser magnitudes, such as hypertension, diabetes or osteoporosis. The focus therefore has been on targets that induce thermogenic adipose tissue, of which the Arb3 pathway with its downstream targets, prominently *C/EBPβ* and *PRDM16*, is most well characterized[19,32-34]. However, agents against these putative targets are not sufficiently developed to be tested in people[19]. Moreover, most such targets, such as *C/EBPβ* and *PPARG*, are expressed ubiquitously and during growth and development, which makes specificity an issue and off-target actions a possibility.

Several considerations make a highly specific Fsh Ab unique. First, it is a dual-acting agent capable of impressively reducing adiposity and improving bone mass. Second, it induces thermogenic adipose tissue to improve whole body metabolism, a likely added benefit for postmenopausal women with disrupted energy homeostasis. Third, it has a powerful action in reducing visceral adiposity. This is clinically very relevant considering that visceral adiposity is associated with an increased risk of metabolic syndrome, coronary artery disease, cancer and diabetes[35]. These complications are thought to arise at least in part from the secretion of proinflammatory cytokines, including IL-6 and TNFα[36]. Fsh blockade could thus be useful not only through its anti-adiposity and thermogenic actions, but also indirectly, *via* its inhibition of

Fsh-induced Tnfα production[37]. Finally, and admittedly speculative, is our premise that an Fsh Ab may have a considerably limited off-target profile, mainly due to the restricted expression of the Fshr in gonads, bone and fat.

ACKNOWLEDGEMENTS

Work at Icahn School of Medicine at Mount Sinai was supported by the National Institutes of Health (NIH) by grants R01 DK80459 (to M.Z. and L.S.), R01 AG40132 (to M.Z.), R01 AG23176 (to M.Z.), R01 AR06592 (to M.Z.) and R01 AR06066 (to M.Z. and N.G.A.). A grant (# 81120108010) from National Science Foundation of China, Ministry of China (International Collaborative Grant to Z.B. and M.Z.) is also gratefully acknowledged. The authors also acknowledge the Medical Research Council-Technology (MRCT), London, UK, as well as Mount Sinai Innovation Partners (MSIP) for their collaboration on the actions of FSH on bone. Work at Maine Medical Center Research Institute was supported by the NIH/NIGMS (P30 GM106391 and P30 GM103392) and the NIH/NIDDK (R24 DK092759-06) to C.J.R. The project was also supported by the Physiology Core Facility grant (P20 GM103465), COBRE in Stem Cell Biology and Regenerative Medicine, a grant supported by the National Institute of General Medical Sciences.

DISCLOSURES

M.Z. is a named inventor on a patent related to FSH and bone, owned by Icahn School of Medicine at Mount Sinai. M.Z. will receive royalties and/or licensing fees *per* Mount Sinai policies, in case the patent is commercialized. M.Z. also consults for Merck, Roche, Novartis, and a number of financial consulting platforms.

LEGENDS TO FIGURES

Figure 1: Ab Blocks Fsh-Fshr Interaction at Physiologic Fsh Concentrations in Plasma. Recombinant mouse Fsh (Fshα-Fshβ chimera, 2 μg) was passed through resin (Pierce Co-Immunoprecipitation Kit, 26149, Thermo Scientific) with immobilized Fsh Ab or goat IgG (**A**). Elution (Eluate), flow-through (Flow), and consecutive wash fractions (Wash) were collected and immunoblotted, as shown, with a different Fsh Ab (Hf2). The sequence of the Fshα-Fshβ chimera is shown (**B**). Peptides from the trypsinized eluate matched by mass spectrometry are marked in red, with the linker peptide shown in red solid circles. Ab was raised against human LVYKDPARPKIQK, which corresponds to mouse LVYKDPARPNTQK (green-filled circles) (B). Crystal structure of the human FSH-FSHR complex (PDB id: 4AY9; FSHα not shown for clarity) indicates that the loop from the FSHβ subunit (yellow), containing the sequence LVYKDPARPKIQK (highlighted as sticks), tucks into a small groove generated by the FSHR (**C**i). Computational modelling of Fsh bearing the peptide sequence LVYKDPARPNTQK shows an identical binding mode (Cii). Positively charged residues (blue) of the peptide surface complements the negatively charged residues (red) of the Fshr binding site, generating strong electrostatic interactions at the binding surface (arrow) (Ciii). Given the small size of the groove (Civ), binding of Ab to the peptide sequence will completely shield Fshβ from entering the Fshr binding pocket. That the Ab blocked Fsh action was confirmed experimentally using dedifferentiated brown adipocytes (Thermo cells), immortalized from the ThermoMouse (Jackson Labs). The latter has a *Luc2-T2A-tdTomato* construct inserted at the initiation codon of the *Ucp1* gene[11] (**D**). Thermo cells retain BAT capacity and report *Ucp1* activation using *Luc2* as

reporter. The effect of Fsh (30 ng/mL) and Fsh Ab (concentrations as noted) on *Ucp1* expression was tested in the absence of fetal bovine serum (that does not contain endogenous FSH) and the Arb3 agonist CL316243 (10^{-7} M). Notably, 1 µg/mL Fsh Ab completely abolished the inhibitory effect of near-circulating levels of Fsh on *Ucp1* expression (**D**) (also see Figures 5E, F). Statistics: comparisons by one-way ANOVA with *posthoc* Bonferroni correction; mean ± SEM; *$P \leq 0.05$, **$P \leq 0.01$; in triplicate). ELISA-based measurements of *goat* IgG/Fsh Ab in *mouse* serum following single injection of Ab at 100 µg (i.p.) yielded serum Ab/IgG concentrations that were 20-fold higher than those required to inhibit Fsh action *in vitro* ($t_{1/2}$ = 25.6 hours). Mean ± SEM, n = 3 mice/group (**E**).

Figure 2: **Fsh Antibody Markedly Reduces White Adipose Tissue and Induces Thermogenesis in Mice Fed on a High Fat Diet.** Daily injection of Fsh antibody (Ab) or goat IgG (200 µg/day/mouse) to 3 month-old male and/or female C57BL/6 mice pair-fed on high fat diet (HFD, see Methods) for up to 8 weeks dramatically decreased fat mass, fat mass/total mass (FM/TM) and increased lean mass/total mass (LM/TM) on quantitative nuclear magnetic resonance (qNMR), without affecting total body weight (**A, B**). Results were confirmed independently using qNMR (**C**) and dual energy X-ray absorptiometry (DXA) (**D**), the latter documenting reduced body fat at 7 weeks, and increased bone mineral density (BMD) at both 4 and 7 weeks. Micro-computed tomography (µCT) of the thoracoabdominal cavity of mice with *ad libitum* access to high fat diet showed a similar marked reduction of total, subcutaneous and visceral fat volume (TFV, SFV and VFV, respectively) (**E**). Representative coronal and transverse sections are shown, where visceral and subcutaneous fat is colored in red and yellow,

respectively (E). Parallel experiments confirmed a reduction in the weight of white, namely inguinal (iWAT) and gonadal (gWAT) adipose fat pads, with no change in interscapular brown adipose tissue (BAT) weight (**F**). Representative images of Oil Red-O-stained sections showing effects of Fsh Ab on fat accumulation in both liver and skeletal muscle (deep red staining) (**G**, liver, x20; muscle x40). Indirect calorimetry using metabolic cages showed significant increases in O_2 utilization (VO_2), energy expenditure (EE), walking distance (walk), walking speed (walk speed), and beam breaks (Xbreaks), with no significant difference in CO_2 production (VCO_2), sleep hours or *ad libitum* food intake (not shown) with Ab *versus* IgG (**H**). Glucose tolerance testing showed no difference between mice receiving IgG or Ab (AUC: area under curve) (**I**). Effect of Ab on plasma C-peptide, adiponectin, and leptin (**J**) levels, as well as on total cholesterol, triglycerides and free fatty acids (**K**). Effects of Ab in reducing fat mass and increasing lean mass (%Δ over ~7 weeks) were near-abolished in *Fshr*$^{-/-}$ mice pair-fed on high fat diet, confirming that Ab action was Fsh-mediated (**L, M**). Statistics: unpaired 2-tailed Student's t-test, assuming equal variance, corrected for Bonferroni, where necessary; *$P \leq 0.05$, **$P \leq 0.01$, or as shown; mean ± SEM; n = 3-12 mice/group.

Figure 3: **Fsh Antibody Reduces Fat Accumulation in Ovariectomized Mice on Normal Chow.** Mice were ovariectomized or sham-operated and injected with Fsh antibody (Ab) or goat IgG (200 or 400 μg/day to sham-operated or ovariectomized mice, respectively) for 8 weeks while on normal chow (see Methods) (**A**). Plasma Fsh levels detected by ELISA (Biotang, M7619) were higher in ovariectomized mice and were not altered with Ab treatment (**B**). Fsh Ab did not affect plasma estrogen (E_2) levels (ELISA,

443 Biotang, M7956) in sham-operated mice; levels mostly fell below assay detection limit in
444 ovariectomized mice. Pair-fed sham and ovariectomized groups showed significant
445 decreases in fat mass, fat mass/total mass (FM/TM) and increases in lean mass/total
446 mass (LM/TM) on quantitative nuclear magnetic resonance (qNMR) (**C**). In separate
447 studies, microcomputed tomography (μCT) of the thoracoabdominal cavity of sham-
448 operated and ovariectomized mice fed *ad libitum* with normal chow similarly showed a
449 marked reduction of total, visceral and subcutaneous fat volume (TFV, VFV and SFV,
450 respectively) (**D**). Representative transverse sections are shown (pink–visceral fat,
451 white–subcutaneous fat) (D). There were also strong reductions in bone marrow fat
452 with the Ab compared with IgG in both sham-operated and ovariectomized groups,
453 noted on osmium μCT (marrow fat shown in white) (**E**). Quantitation of marrow fat area
454 (MA)/total volume (TV) at three voxels of interest (VOI) is shown (E). Indirect
455 calorimetry using metabolic cages was consistent with an Ab-induced thermogenic
456 response, notably increases in energy expenditure (EE) (resting and/or active) and
457 physical activity (wheel meters), with decreased respiratory quotient (RQ) (**F**). Plasma
458 glucose, total cholesterol, triglyceride and free fatty acids remained unchanged with Ab
459 (**G**). Statistics: Comparisons by unpaired 2-tailed Student's t-test or one-way ANOVA,
460 assuming equal variance, and corrected for Bonferroni where necessary; *$P \leq 0.05$,
461 **$P \leq 0.01$, or as show; mean ± SEM; n = 4-10 mice/group).
462
463 **Figure 4: Fsh Ab Reduces Body Fat in Mice Fed on Normal Chow.** Three month-
464 old C56BL/6 female mice were either pair-fed (**A-C**) or reverse pair-fed with normal
465 chow (**D-F**) and injected with Fsh Ab or IgG (100 μg/mouse/day) for 7 and 5 weeks,

466 respectively. For pair-feeding, the amount of chow consumed *ad libitum* by the IgG
467 group was given to the Ab-treated group. For the reverse pair-feeding, the Ab-treated
468 group was allowed *ad libitum* access to food and the same amount of chow was given
469 to IgG group, with the left-over chow measured to determine food intake of the IgG
470 group (see Methods). A significant increase in food intake by Ab-treated mice was
471 noted in the reverse pair-feeding protocol (D). Nonetheless, as with mice on a high fat
472 diet (*c.f.* Figure 2B, C), in either feeding protocol, Ab caused a significant decrease in fat
473 mass and fat mass/total mass (FM/TM) and increase in lean mass/total mass (LM/TM)
474 on quantitative nuclear magnetic resonance (qNMR) (B and E), but without an effect on
475 total body weight (A and D). Micro-computed tomography (μCT) showed profound
476 decrements in thoracoabdominal fat, visualized in representative coronal and transverse
477 sections (red–visceral fat; yellow–subcutaneous fat), and upon quantitation of total,
478 subcutaneous and visceral fat volumes (TFV, SFV and VFV, respectively) (C and F).
479 Statistics: Unpaired 2-tailed Student's t-test, assuming equal variance, and corrected for
480 Bonferroni where necessary; *$P \leq 0.05$, **$P \leq 0.01$, or as shown (n = 4-5 mice/group).
481
482 **Figure 5**: **Ab Blocks Fsh Effects on Signaling-Efficient Fshrs to Activate *Ucp1*.**
483 Western immunoblotting shows the presence of Fsh receptors (Fshr) in 3T3.L1 cells,
484 dedifferentiated brown adipocytes (Thermo cells), mesenchymal stem cell-derived
485 adipocytes (MSC-adipocytes), and HeLa cells, but not on fibroblasts (293T) (**A**).
486 Sanger sequencing confirmed full length Fshr cDNA in 3T3.L1 cells and MSC-
487 adipocytes (see Extended Data Figure 1). Strong immunostaining with an anti-Fshr
488 antibody (Lifespan Bioscience, LS-A4004) of sections of inguinal WAT and visceral

WAT (iWAT and vWAT, respectively) and BAT from C57BL/6 mice fed on normal chow (**B**). Effect of Fsh (30 ng/mL) on the expression of core lipogenic genes, namely *Ppparg*, *Fas*, *Glut4*, *Lpl*, *Pref1*, *Cebpd*, and *Lep* in 3T3.L1 cells (**C**). MSC-adipocytes from *Fshr*$^{-/-}$ mice showed reduced Oil Red-O staining (also quantitated calorimetrically in isopropanol cell extracts) *versus* cells from wild type littermates (**D**). Luc2 activity was measured in extracts of Thermo cells (Figure 1D) (cultured in the presence of fetal bovine serum containing Fsh) in response to Ab (100 ng/mL) with/without the Arb3 agonist CL316243 (10^{-7} M) (**E**). The same cells ($1.5x10^{6}$) were implanted into each flank of *nu/nu* mice, which were fed on normal chow and injected with Ab (200 µg/mouse/day) for 8 weeks, following which Luc2 radiance was quantitated post D-Luciferin (10 µL/g) injection, using an IVIS luminescence imager (**F**) (see Methods). For confirmation, sections of resected areas where cells had been implanted were examined for *tdTomato* fluorescence (x20) (**G**).

Figure 6: **Fsh Ab Induces Thermogenic Adipose Tissue in Mice on a High Fat Diet.** Representative hematoxylin/eosin (H&E) stained sections of inguinal white adipose tissue (iWAT) showing white-to-beige transition of adipocytes upon daily injection for 8 weeks of Fsh antibody (Ab) or goat IgG (200 µg/mouse) to 3 month-old C57BL/6 mice pair-fed on high fat diet. Morphometry yielded highly significant reductions in adipocyte area and perimeter (**A**). Immunolabeling for Ucp1 showed more intense staining in both iWAT and interscapular brown adipose tissue (BAT) (**B**) (representative sections, scale shown). Shown also is the relative expression of the genes (names noted) in BAT *versus* WAT (**C**i). Consistent with adipocyte beiging was an enhancement of BAT gene

512 expression (qPCR) in iWAT at 1 and/or 3 months (M) (Cii). Statistics: Unpaired 2-tailed
513 Student's t-test, assuming equal variance, corrected for Bonferroni, where required;
514 *$P \leq 0.05$, **$P \leq 0.01$ (qPCR, 3 biological replicates *per* group, each measured in
515 triplicate).
516
517 **Figure 7**: **Fsh Ab Triggers Early *Ucp1* Expression and Enhances Cellular**
518 **Mitochondrial Density *In Vivo*.** In the ThermoMouse, a luciferase reporter construct,
519 *Luc2-T2A-tdTomato*, is inserted into the *Ucp1* locus on the Y-chromosome (see Figure
520 1D)[11]. Activation of *Ucp1* expression leads to upregulation of *Luc2*, which can be
521 quantitated *in vivo* by radiance measurements, using IVIS, following the injection of D-
522 Luciferin (10 µL/g) (see Methods). 3 month-old male ThermoMice were treated with Fsh
523 antibody (Ab) or goat IgG (200 µg/mouse) for 2 (**A**) or 8 weeks (**B**) while being pair-fed
524 on high fat diet, followed by D-Luciferin injection and radiance capture from dorsal
525 and/or ventral surfaces of the entire body (total), inguinal white adipose tissue (WAT),
526 and interscapular brown adipose tissue (BAT) regions. Dramatic increases were noted
527 in all parameters with the Ab compared with IgG or no treatment (Ctrl). Of note is that,
528 at two weeks, there was increased BAT, but not iWAT radiance, suggesting early
529 activation of *Ucp1* in BAT. To assess mitochondrial density, we used the PhAM^{excised}
530 mouse, wherein fluorescent dendra2 is selectively localized to mitochondria using a
531 *Cox8* mitochondrial targeting signal[23]. Injection of Ab for 2 weeks in mice fed on normal
532 chow dramatically increased dendra2 green fluorescence in the subcutaneous WAT
533 (sWAT), visceral WAT (vWAT), and BAT compartments. Statistics: Comparison of Ab

versus IgG by unpaired 2-tailed Student's t-test, assuming equal variance; *P* values shown.

REFERENCES

1 Sun, L. *et al.* FSH directly regulates bone mass. *Cell* **125**, 247-260, doi:10.1016/j.cell.2006.01.051 (2006).

2 Randolph, J. F., Jr. *et al.* The value of follicle-stimulating hormone concentration and clinical findings as markers of the late menopausal transition. *J Clin Endocrinol Metab* **91**, 3034-3040, doi:10.1210/jc.2006-0243 (2006).

3 Sowers, M. R. *et al.* Endogenous hormones and bone turnover markers in pre- and perimenopausal women: SWAN. *Osteoporos Int* **14**, 191-197, doi:10.1007/s00198-002-1329-4 (2003).

4 Thurston, R. C. *et al.* Gains in body fat and vasomotor symptom reporting over the menopausal transition: the study of women's health across the nation. *Am J Epidemiol* **170**, 766-774, doi:10.1093/aje/kwp203 (2009).

5 Riggs, B. L., Khosla, S. & Melton, L. J., 3rd. A unitary model for involutional osteoporosis: estrogen deficiency causes both type I and type II osteoporosis in postmenopausal women and contributes to bone loss in aging men. *J Bone Miner Res* **13**, 763-773, doi:10.1359/jbmr.1998.13.5.763 (1998).

6 Van Pelt, R. E., Gavin, K. M. & Kohrt, W. M. Regulation of Body Composition and Bioenergetics by Estrogens. *Endocrinol Metab Clin North Am* **44**, 663-676, doi:10.1016/j.ecl.2015.05.011 (2015).

7 Zhu, L. L. *et al.* Blocking antibody to the beta-subunit of FSH prevents bone loss by inhibiting bone resorption and stimulating bone synthesis. *Proc Natl Acad Sci U S A* **109**, 14574-14579, doi:10.1073/pnas.1212806109 (2012).

8 Zhu, L. L. *et al.* Blocking FSH action attenuates osteoclastogenesis. *Biochem Biophys Res Commun* **422**, 54-58, doi:10.1016/j.bbrc.2012.04.104 (2012).

9 Cohen, P. & Spiegelman, B. M. Brown and Beige Fat: Molecular Parts of a Thermogenic Machine. *Diabetes* **64**, 2346-2351, doi:10.2337/db15-0318 (2015).

10 Cypess, A. M. & Kahn, C. R. Brown fat as a therapy for obesity and diabetes. *Curr Opin Endocrinol Diabetes Obes* **17**, 143-149, doi:10.1097/MED.0b013e328337a81f (2010).

11 Galmozzi, A. *et al.* ThermoMouse: an in vivo model to identify modulators of UCP1 expression in brown adipose tissue. *Cell Rep* **9**, 1584-1593, doi:10.1016/j.celrep.2014.10.066 (2014).

12 Danilovich, N. *et al.* Estrogen deficiency, obesity, and skeletal abnormalities in follicle-stimulating hormone receptor knockout (FORKO) female mice. *Endocrinology* **141**, 4295-4308, doi:10.1210/endo.141.11.7765 (2000).

13 Jones, M. E. *et al.* Aromatase-deficient (ArKO) mice accumulate excess adipose tissue. *J Steroid Biochem Mol Biol* **79**, 3-9 (2001).

14 Lindberg, M. K. *et al.* Estrogen receptor specificity for the effects of estrogen in ovariectomized mice. *J Endocrinol* **174**, 167-178 (2002).

15 Liu, X. M. *et al.* FSH regulates fat accumulation and redistribution in aging through the Galphai/Ca(2+)/CREB pathway. *Aging Cell* **14**, 409-420, doi:10.1111/acel.12331 (2015).

16 Cui, H. *et al.* FSH stimulates lipid biosynthesis in chicken adipose tissue by upregulating the expression of its receptor FSHR. *J Lipid Res* **53**, 909-917, doi:10.1194/jlr.M025403 (2012).

17 Wu, J., Cohen, P. & Spiegelman, B. M. Adaptive thermogenesis in adipocytes: is beige the new brown? *Genes Dev* **27**, 234-250, doi:10.1101/gad.211649.112 (2013).

18 Jimenez, M. *et al.* Validation of an ultrasensitive and specific immunofluorometric assay for mouse follicle-stimulating hormone. *Biol Reprod* **72**, 78-85, doi:10.1095/biolreprod.104.033654 (2005).

19 Giordano, A., Frontini, A. & Cinti, S. Convertible visceral fat as a therapeutic target to curb obesity. *Nat Rev Drug Discov* **15**, 405-424, doi:10.1038/nrd.2016.31 (2016).

20 Wu, J. *et al.* Beige adipocytes are a distinct type of thermogenic fat cell in mouse and human. *Cell* **150**, 366-376, doi:10.1016/j.cell.2012.05.016 (2012).

21 Cedikova, M. *et al.* Mitochondria in White, Brown, and Beige Adipocytes. *Stem Cells Int* **2016**, 6067349, doi:10.1155/2016/6067349 (2016).

22 Shabalina, I. G. *et al.* UCP1 in brite/beige adipose tissue mitochondria is functionally thermogenic. *Cell Rep* **5**, 1196-1203, doi:10.1016/j.celrep.2013.10.044 (2013).

23 Pham, A. H., McCaffery, J. M. & Chan, D. C. Mouse lines with photo-activatable mitochondria to study mitochondrial dynamics. *Genesis* **50**, 833-843, doi:10.1002/dvg.22050 (2012).

24 Abe, E. *et al.* TSH is a negative regulator of skeletal remodeling. *Cell* **115**, 151-162 (2003).

25 Zaidi, M. Skeletal remodeling in health and disease. *Nat Med* **13**, 791-801, doi:10.1038/nm1593 (2007).

26 Zaidi, M. *et al.* ACTH protects against glucocorticoid-induced osteonecrosis of bone. *Proc Natl Acad Sci U S A* **107**, 8782-8787, doi:10.1073/pnas.0912176107 (2010).

27 Sun, L. *et al.* Functions of vasopressin and oxytocin in bone mass regulation. *Proc Natl Acad Sci U S A* **113**, 164-169, doi:10.1073/pnas.1523762113 (2016).

28 Tamma, R. *et al.* Oxytocin is an anabolic bone hormone. *Proc Natl Acad Sci U S A* **106**, 7149-7154, doi:10.1073/pnas.0901890106 (2009).

29 Tamma, R. *et al.* Regulation of bone remodeling by vasopressin explains the bone loss in hyponatremia. *Proc Natl Acad Sci U S A* **110**, 18644-18649, doi:10.1073/pnas.1318257110 (2013).

30 Blair, H. C. *et al.* Skeletal receptors for steroid-family regulating glycoprotein hormones: A multilevel, integrated physiological control system. *Ann N Y Acad Sci* **1240**, 26-31, doi:10.1111/j.1749-6632.2011.06287.x (2011).

31 Kawai, H., Furuhashi, M. & Suganuma, N. Serum follicle-stimulating hormone level is a predictor of bone mineral density in patients with hormone replacement therapy. *Arch Gynecol Obstet* **269**, 192-195, doi:10.1007/s00404-003-0532-7 (2004).

32 Cinti, S. Adipose tissues and obesity. *Ital J Anat Embryol* **104**, 37-51 (1999).

33 Jimenez, M. *et al.* Beta 3-adrenoceptor knockout in C57BL/6J mice depresses the occurrence of brown adipocytes in white fat. *Eur J Biochem* **270**, 699-705 (2003).

34 Cohen, P. *et al.* Ablation of PRDM16 and beige adipose causes metabolic dysfunction and a subcutaneous to visceral fat switch. *Cell* **156**, 304-316, doi:10.1016/j.cell.2013.12.021 (2014).

35 Despres, J. P. & Lemieux, I. Abdominal obesity and metabolic syndrome. *Nature* **444**, 881-887, doi:10.1038/nature05488 (2006).

36 Smith, U. Abdominal obesity: a marker of ectopic fat accumulation. *J Clin Invest* **125**, 1790-1792, doi:10.1172/JCI81507 (2015).

37 Iqbal, J., Sun, L., Kumar, T. R., Blair, H. C. & Zaidi, M. Follicle-stimulating hormone stimulates TNF production from immune cells to enhance osteoblast and osteoclast formation. *Proc Natl Acad Sci U S A* **103**, 14925-14930, doi:10.1073/pnas.0606805103 (2006).

Fig 1

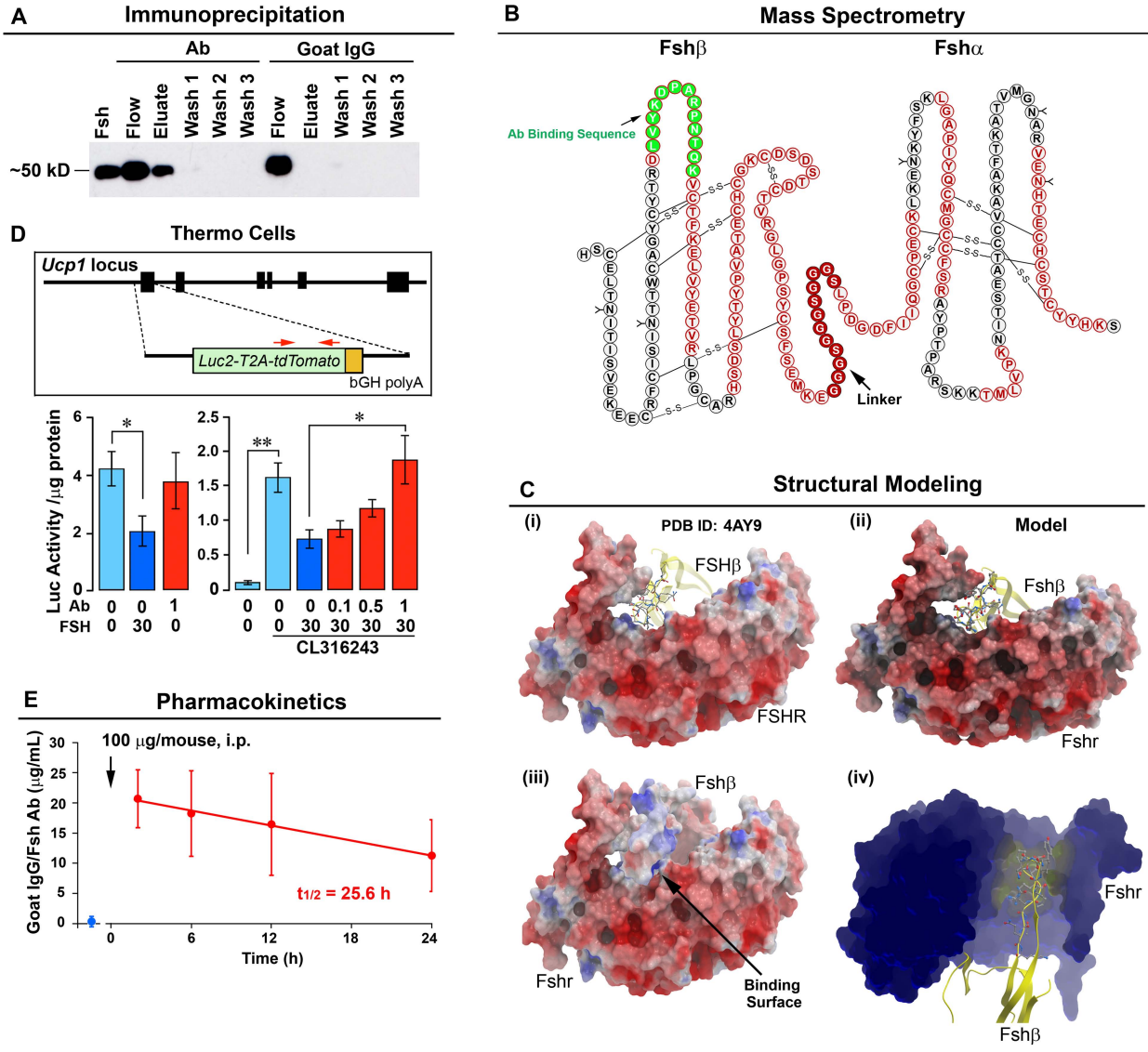
A
Immunoprecipitation
Ab
Goat IgG
Fsh
Flow
Eluate
Wash 1
Wash 2
Wash 3
Flow
Eluate
Wash 1
Wash 2
Wash 3
~50 kD
B
Mass Spectrometry
Fshβ
Fshα
Ab Binding Sequence
Linker
C
Structural Modeling
(i)
PDB ID: 4AY9
FSHβ
FSHR
(ii)
Model
Fshβ
Fshr
(iii)
Fshβ
Fshr
Binding Surface
(iv)
Fshr
Fshβ
D
Thermo Cells
Ucp1 locus
Luc2-T2A-tdTomato
bGH polyA
Luc Activity /μg protein
Ab
FSH
CL316243
E
Pharmacokinetics
100 μg/mouse, i.p.
Goat IgG/Fsh Ab (μg/mL)
t1/2 = 25.6 h
Time (h)

Fig 2

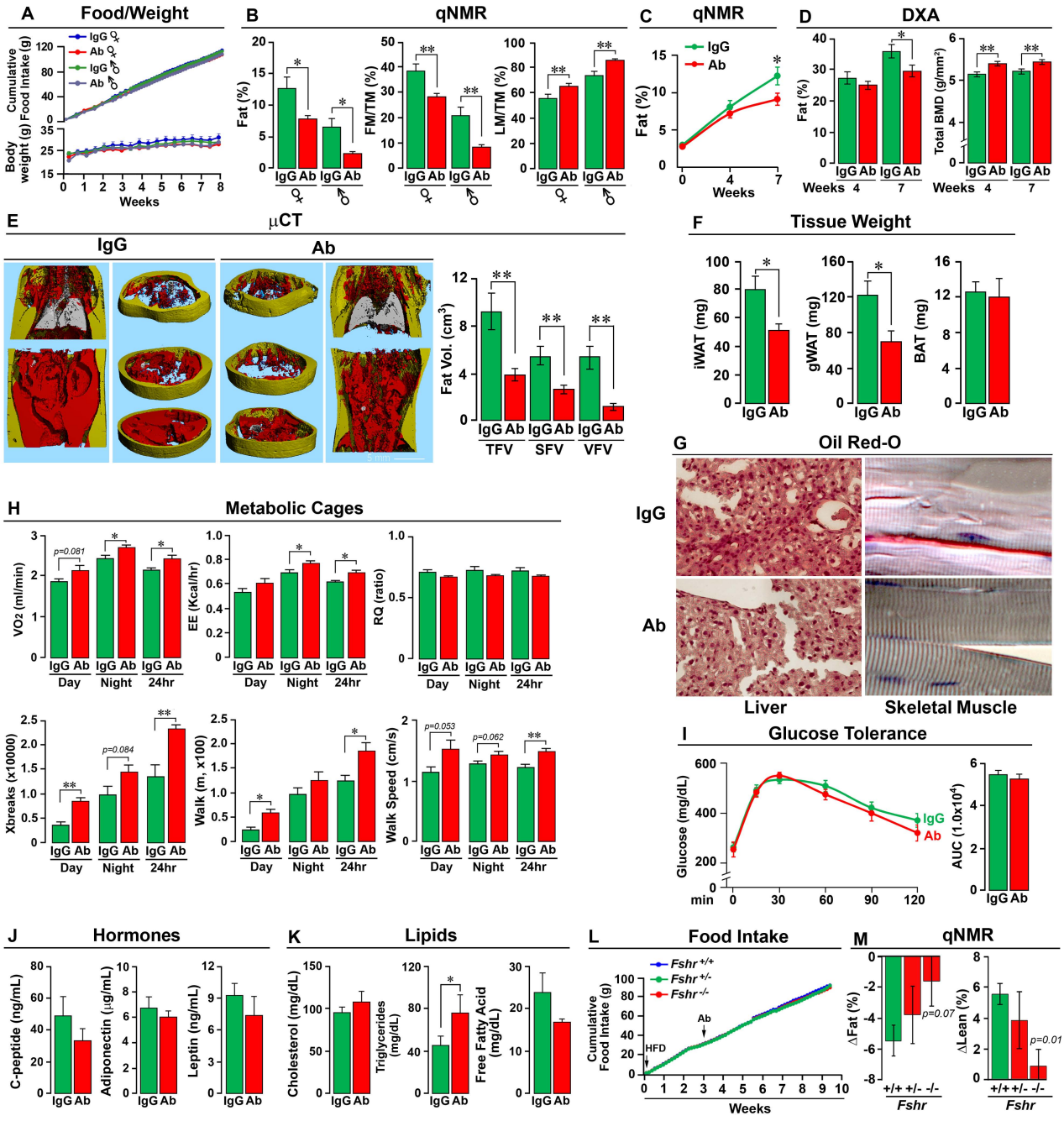
A
Food/Weight
IgG ♀
Ab ♀
IgG ♂
Ab ♂
Cumulative Food Intake (g)
Body weight (g)
Weeks
B
qNMR
Fat (%)
FM/TM (%)
LM/TM (%)
IgG Ab
C
qNMR
IgG
Ab
Fat (%)
Weeks
D
DXA
Fat (%)
Total BMD (g/mm²)
Weeks 4 7
E
μCT
IgG
Ab
Fat Vol. (cm³)
TFV SFV VFV
F
Tissue Weight
iWAT (mg)
gWAT (mg)
BAT (mg)
G
Oil Red-O
IgG
Ab
Liver
Skeletal Muscle
H
Metabolic Cages
VO₂ (ml/min)
EE (Kcal/hr)
RQ (ratio)
Xbreaks (x10000)
Walk (m, x100)
Walk Speed (cm/s)
p=0.081
p=0.084
p=0.053
p=0.062
Day Night 24hr
I
Glucose Tolerance
Glucose (mg/dL)
min
AUC (1.0x10⁴)
J
Hormones
C-peptide (ng/mL)
Adiponectin (μg/mL)
Leptin (ng/mL)
K
Lipids
Cholesterol (mg/dL)
Triglycerides (mg/dL)
Free Fatty Acid (mg/dL)
L
Food Intake
Fshr+/+
Fshr+/-
Fshr-/-
HFD
Ab
Cumulative Food Intake (g)
Weeks
M
qNMR
ΔFat (%)
ΔLean (%)
p=0.07
p=0.01
+/+ +/- -/-
Fshr

Fig 3

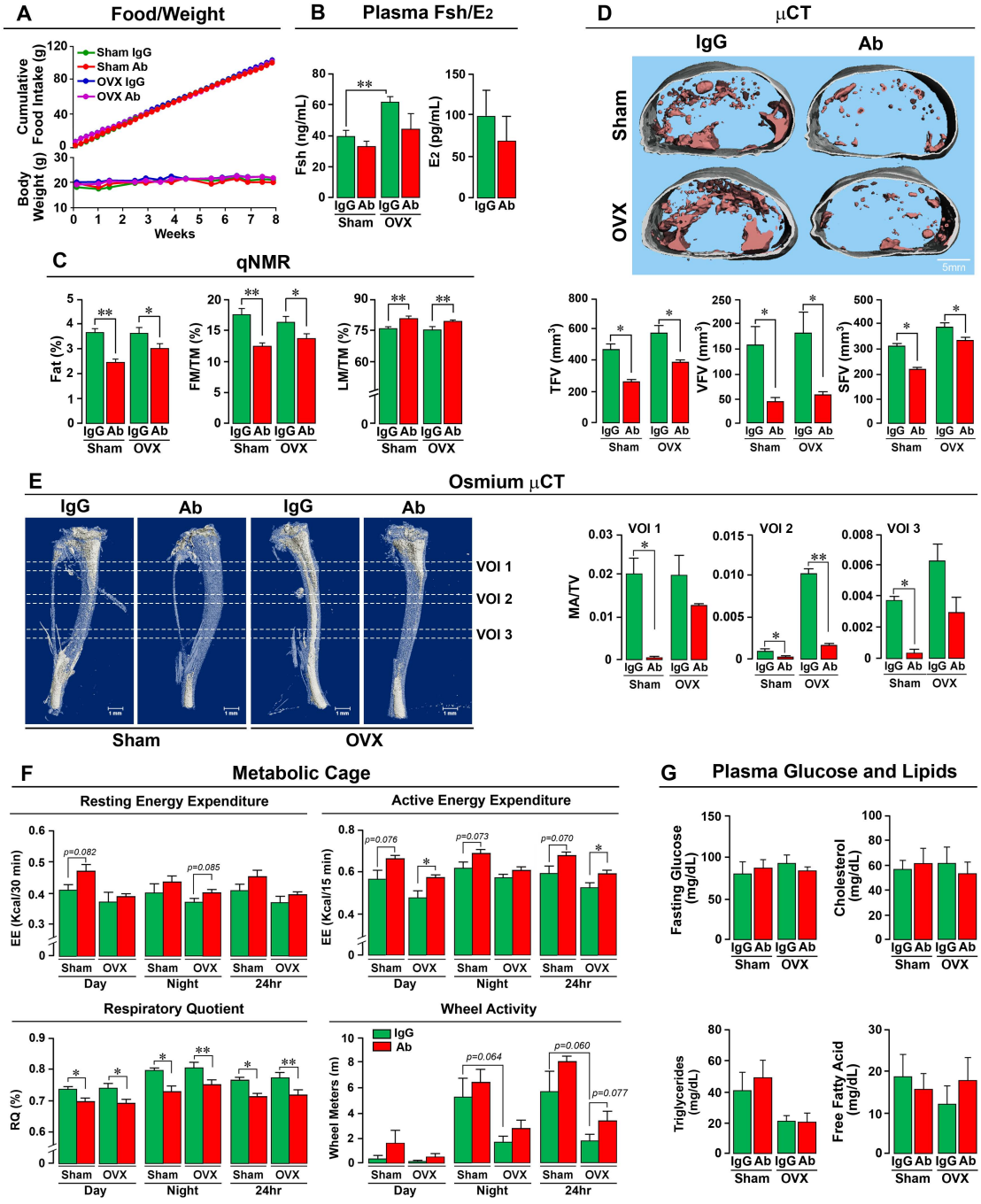
A
Food/Weight
Sham IgG
Sham Ab
OVX IgG
OVX Ab
Cumulative Food Intake (g)
Body Weight (g)
Weeks
B
Plasma Fsh/E2
Fsh (ng/mL)
E2 (pg/mL)
IgG Ab IgG Ab
Sham OVX
C
qNMR
Fat (%)
FM/TM (%)
LM/TM (%)
D
μCT
IgG
Ab
Sham
OVX
5mm
TFV (mm3)
VFV (mm3)
SFV (mm3)
E
Osmium μCT
VOI 1
VOI 2
VOI 3
MA/TV
F
Metabolic Cage
Resting Energy Expenditure
Active Energy Expenditure
EE (Kcal/30 min)
EE (Kcal/15 min)
Day
Night
24hr
Respiratory Quotient
RQ (%)
Wheel Activity
Wheel Meters (m)
G
Plasma Glucose and Lipids
Fasting Glucose (mg/dL)
Cholesterol (mg/dL)
Triglycerides (mg/dL)
Free Fatty Acid (mg/dL)

Fig 4

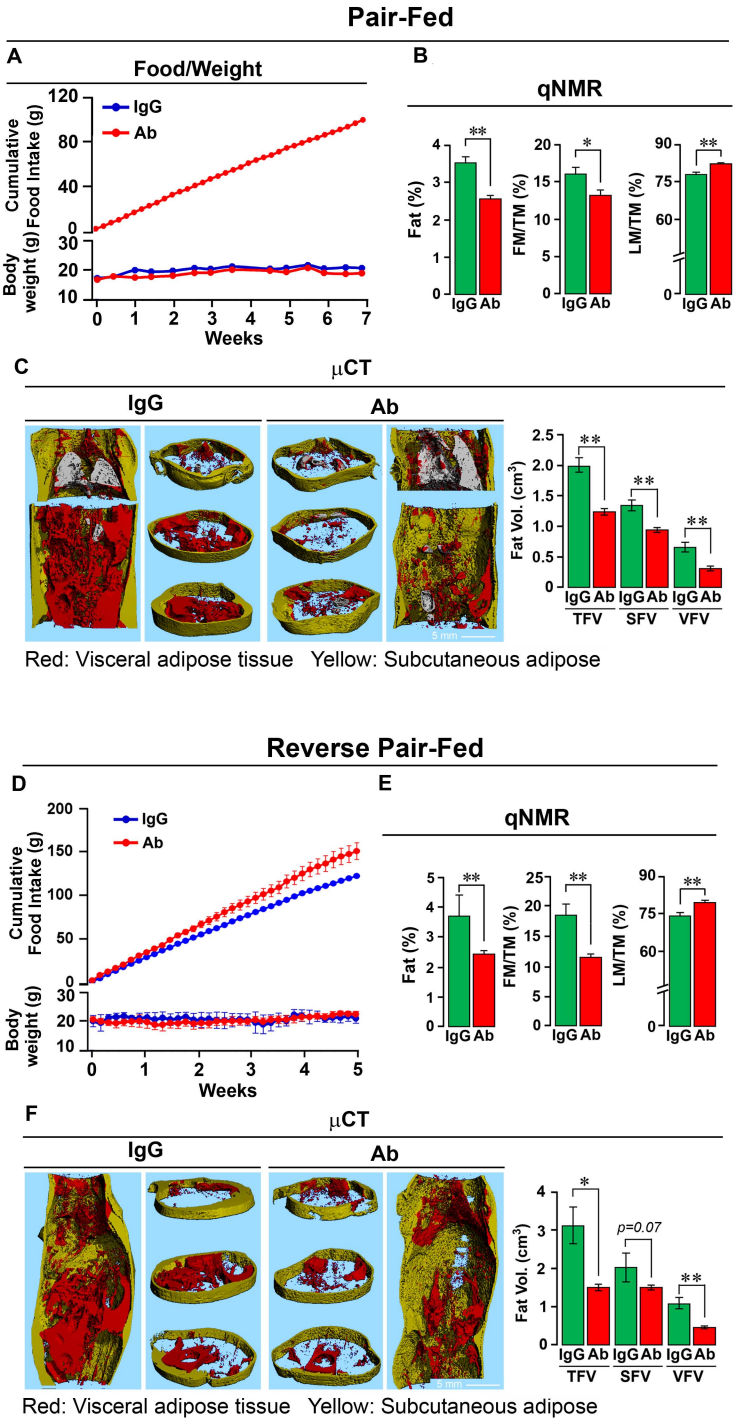
Pair-Fed
A
Food/Weight
IgG
Ab
Cumulative Food Intake (g)
Body weight (g)
Weeks
B
qNMR
Fat (%)
FM/TM (%)
LM/TM (%)
C
μCT
IgG
Ab
Fat Vol. (cm³)
TFV
SFV
VFV
Red: Visceral adipose tissue Yellow: Subcutaneous adipose
Reverse Pair-Fed
D
E
F
p=0.07

Fig 5

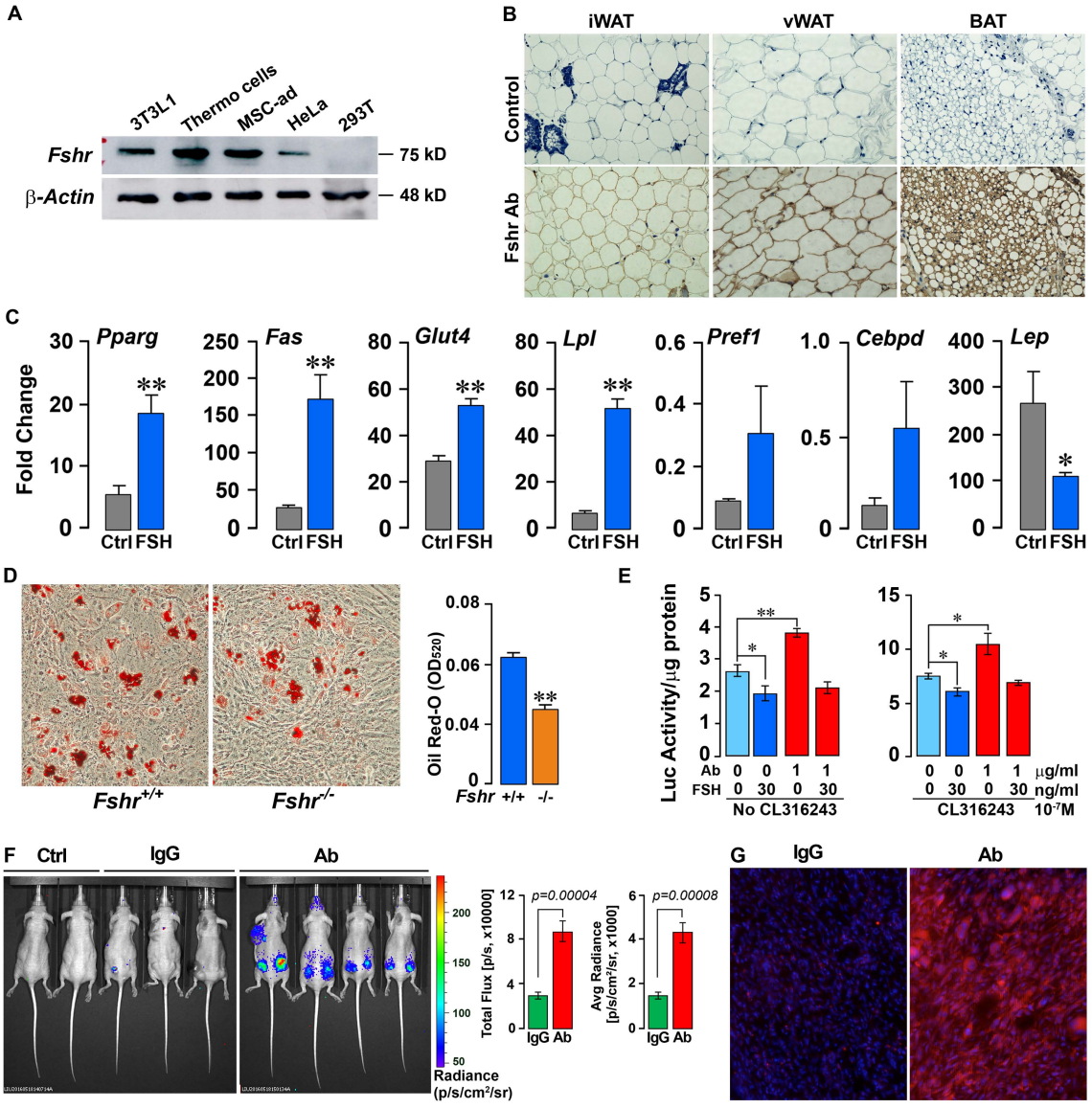
A
3T3L1
Thermo cells
MSC-ad
HeLa
293T
Fshr
β-Actin
75 kD
48 kD
B
iWAT
vWAT
BAT
Control
Fshr Ab
C
Fold Change
Pparg
Fas
Glut4
Lpl
Pref1
Cebpd
Lep
Ctrl FSH
D
Fshr+/+
Fshr-/-
Oil Red-O (OD520)
Fshr +/+ -/-
E
Luc Activity/μg protein
Ab
FSH
No CL316243
CL316243
μg/ml
ng/ml
10-7M
F
Ctrl
IgG
Ab
Radiance (p/s/cm2/sr)
Total Flux [p/s, x10000]
Avg Radiance [p/s/cm2/sr, x1000]
p=0.00004
p=0.00008
G
IgG
Ab

Fig 6

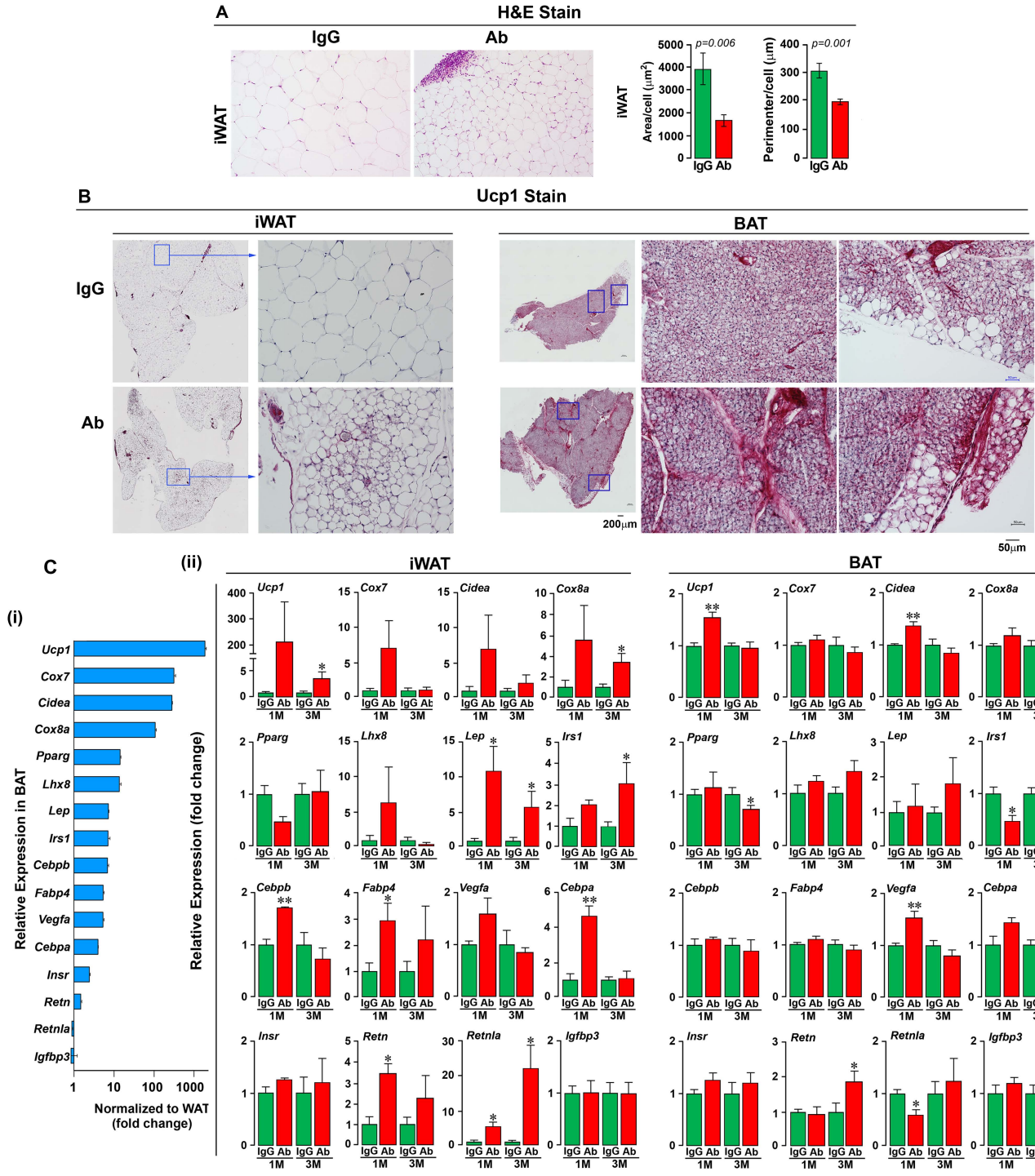
A
H&E Stain
IgG
Ab
iWAT
p=0.006
p=0.001
Area/cell (μm²)
Perimenter/cell (μm)
IgG Ab
B
Ucp1 Stain
iWAT
BAT
IgG
Ab
200μm
50μm
C
(i)
Ucp1
Cox7
Cidea
Cox8a
Pparg
Lhx8
Lep
Irs1
Cebpb
Fabp4
Vegfa
Cebpa
Insr
Retn
Retnla
Igfbp3
Relative Expression in BAT
Normalized to WAT (fold change)
(ii)
Relative Expression (fold change)
1M
3M

Fig 7

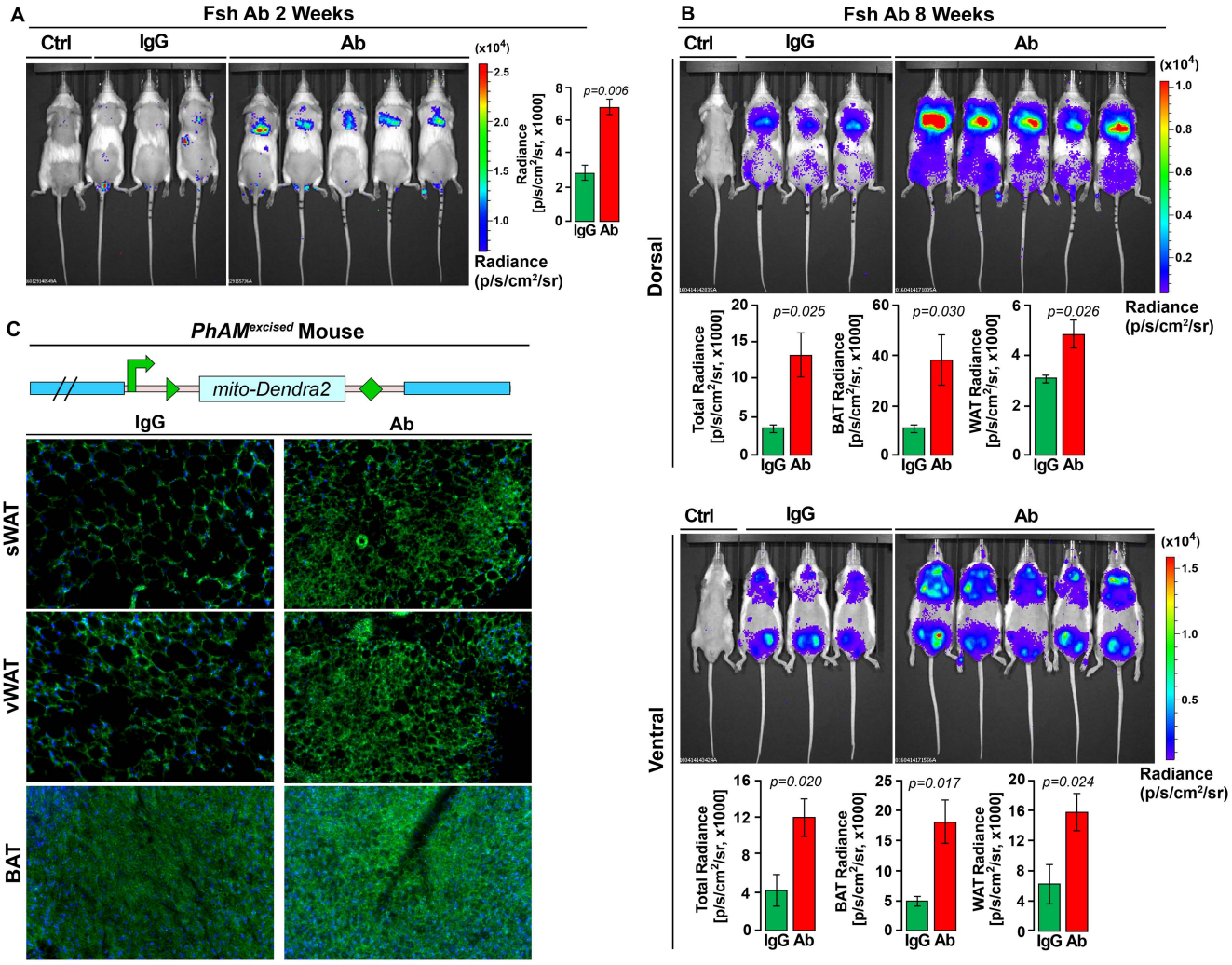
A
Fsh Ab 2 Weeks
Ctrl
IgG
Ab
(x10^4)
2.5
2.0
1.5
1.0
Radiance (p/s/cm²/sr)
Radiance [p/s/cm²/sr, x1000]
p=0.006
IgG Ab
B
Fsh Ab 8 Weeks
Dorsal
Ventral
Total Radiance [p/s/cm²/sr, x1000]
p=0.025
BAT Radiance [p/s/cm²/sr, x1000]
p=0.030
WAT Radiance [p/s/cm²/sr, x1000]
p=0.026
p=0.020
p=0.017
p=0.024
C
PhAM^excised Mouse
mito-Dendra2
sWAT
vWAT
BAT